High-order harmonic generation in polar media induced by chirped few-cycle pulses

Pidong Hu,[1] **Yueping Niu,**[1,3] **Shangqing Gong,**[1,4] **and Chengpu Liu**[2,*]

[1]*Department of Physics, East China University of Science and Technology, Meilong Road 130, Shanghai 200237, China*
[2]*State Key Laboratory of High Field Laser Physics, Shanghai Institute of Optics and Fine Mechanics, Chinese Academy of Sciences, Qinghe Road 390, Shanghai 201800, China*
[3]*niuyp@ecust.edu.cn*
[4]*sqgong@ecust.edu.cn*
**chpliu@siom.ac.cn*

Abstract: The high-order harmonic generation in a polar medium (a medium with a permanent dipole moment) driven by a chirped few-cycle laser pulse is investigated via numerically solving the nonlinear Bloch equations or Maxwell-Bloch equations if taking the propagation effect into account. The time-frequency characteristic of the harmonic is analyzed by means of the wavelet transform of induced time-dependent dipole moment. The simulation results demonstrate that, the harmonic cutoff energy can be dramatically extended as a result of the existence of the permanent dipole moment, and the quantum trajectory number for plateau harmonics can be largely reduced due to the introduce of chirps. Correspondingly, an attosecond pulse pair (APP) can be generated. Moreover, the propagation effect can make the APP's intensity enhanced by one order at a suitable propagation distance, and the latter can be modulated by changing the medium's density.

OCIS codes: (140.7090) Ultralfast lasers; (190.4180) Multiphoton processes; (320.7110) Ultrafast nonlinear optics; (190.5530) Pulse propagation and solitons.

References and links

1. A. Mokhtari, P. Cong, J. L. Herek, and A. H. Zewail, "Direct femtosecond mapping of trajectories in a chemical reaction," Nature **348**, 225–227 (1990).
2. T. Ergler, B. Feuerstein, A. Rudenko, K. Zrost, C. D. Schröter, R. Moshammer, and J. Ullrich, "Quantum-phase resolved mapping of ground-state vibrational D_2 wave packets via selective depletion in intense laser pulses," Phys. Rev. Lett. **97**, 103004 (2006).
3. M. Uiberacker, T. Uphues, M. Schultze, A. J. Verhoef, V. Yakovlev, M. F. Kling, J. Rauschenberger, N. M. Kabachnik, H. Schroder, M. Lezius, K. L. Kompa, H. G. Muller, M. J. J. Vrakking, S. Hendel, U. Kleineberg, U. Heinzmann, M. Drescher, and F. Krausz, "Attosecond real-time observation of electron tunnelling in atoms," Nature **446**, 627–632 (2007).
4. F. Krausz and M. Ivanov, "Attosecond physics," Rev. Mod. Phys. **81**, 163–234 (2009).
5. B. W. Shore and P. L. Knight, "Enhancement of high optical harmonics by excess-photon ionisation," J. Phys. B: At. Mol. Opt. Phys. **20**, 413 (1987).
6. A. McPherson, G. Gibson, H. Jara, U. Johann, T. S. Luk, I. A. McIntyre, K. Boyer, and C. K. Rhodes, "Studies of multiphoton production of vacuum-ultraviolet radiation in the rare gases," J. Opt. Soc. Am. B **4**, 595–601 (1987).
7. M. Ferray, A. L'Huillier, X. F. Li, L. A. Lompre, G. Mainfray, and C. Manus, "Multiple-harmonic conversion of 1064 nm radiation in rare gases," J. Phys. B: At. Mol. Opt. Phys. **21**, L31 (1988).

8. P. B. Corkum, "Plasma perspective on strong field multiphoton ionization," Phys. Rev. Lett. **71**, 1994–1997 (1993).
9. M. Lewenstein, P. Balcou, M. Y. Ivanov, A. L'Huillier, and P. B. Corkum, "Theory of high-harmonic generation by low-frequency laser fields," Phys. Rev. A **49**, 2117–2132 (1994).
10. M. Protopapas, C. H. Keitel, and P. L. Knight, "Atomic physics with super-high intensity lasers," Rep. Prog. Phys. **60**, 389–486 (1997).
11. B. Sundaram and P. W. Milonni, "High-order harmonic generation: simplified model and relevance of single-atom theories to experiment," Phys. Rev. A **41**, 6571–6573 (1990).
12. M. Y. Ivanov and P. B. Corkum, "Generation of high-order harmonics from inertially confined molecular ions," Phys. Rev. A **48**, 580–590 (1993).
13. A. E. Kaplan and P. L. Shkolnikov, "Superdressed two-level atom: very high harmonic generation and multiresonances," Phys. Rev. A **49**, 1275–1280 (1994).
14. F. I. Gauthey, B. M. Garraway, and P. L. Knight, "High harmonic generation and periodic level crossings," Phys. Rev. A **56**, 3093–3096 (1997).
15. C. Figueira de Morisson Faria and I. Rotter, "High-order harmonic generation in a driven two-level atom: periodic level crossings and three-step processes," Phys. Rev. A **66**, 013402 (2002).
16. G. Sansone, E. Benedetti, F. Calegari, C. Vozzi, L. Avaldi, R. Flammini, L. Poletto, P. Villoresi, C. Altucci, R. Velotta, S. Stagira, S. De Silvestri, and M. Nisoli, "Isolated single-cycle attosecond pulses," Science **314**, 443–446 (2006).
17. J. J. Carrera and S.-I. Chu, "Extension of high-order harmonic generation cutoff via coherent control of intense few-cycle chirped laser pulses," Phys. Rev. A **75**, 033807 (2007).
18. Z. Zeng, Y. Cheng, X. Song, R. Li, and Z. Xu, "Generation of an extreme ultraviolet supercontinuum in a two-color laser field," Phys. Rev. Lett. **98**, 203901 (2007).
19. Z. Chang, "Controlling attosecond pulse generation with a double optical gating," Phys. Rev. A **76**, 051403 (2007).
20. S. Gong, Z. Wang, S. Du, and Z. Xu, "Coherent control of high-order harmonic generation in a two-level atom driven by intense two-colour laser fields," J. Mod. Opt. **46**, 1669–1676 (1999).
21. Z. Wang, S. Gong, and Z. Xu, "Attosecond light pulse generation in a strongly driven two-level atom," Acta Phys. Sin. **48**, 961–965 (1999).
22. C. Liu, S. Gong, R. Li, and Z. Xu, "Coherent control in the generation of harmonics and hyper-Raman lines from a strongly driven two-level atom," Phys. Rev. A **69**, 023406 (2004).
23. W. Yang, S. Gong, R. Li and Z. Xu, "Generation of attosecond pulses in a system with permanent dipole moment," Phys. Lett. A **362**, 37–41 (2007).
24. N. Cui, Y. Xiang, Y. Niu, and S. Gong, "Coherent control of terahertz harmonic generation by a chirped few-cycle pulse in a quantum well," New J. Phys. **12**, 013009 (2010).
25. Le Kien, Fam Midorikawa, Katsumi Suda, and Akira, "Attosecond pulse generation using high harmonics in the multicycle regime of the driver pulse," Phys. Rev. A **58**(4), 3311–3319 (1998).
26. Yongli Yu, Xiaohong Song, Yuxi Fu, Ruxin Li, Ya Cheng, and Zhizhan Xu, "Theoretical investigation of single attosecond pulse generation in an orthogonally polarized two-color laser field," Opt. Express **16**(2), 686–694 (2008).
27. Qingbin Zhang, Peixiang Lu, Pengfei Lan, Weiyi Hong, and Zhenyu Yang, "Multi-cycle laser-driven broadband supercontinuum with a modulated polarization gating," Opt. Express **16**(13), 9795–9803 (2008).
28. Yang Xiang, Yueping Niu, and Shangqing Gong, "Proposal for isolated-attosecond-pulse generation in the multicycle regime through modulation of the carrier wave," Phys. Rev. A **85**(2), 023808 (2012).
29. Y. Mairesse, A. de Bohan, L. J. Frasinski, H. Merdji, L. C. Dinu, P. Monchicourt, P. Breger, M. Kovačev, R. Taïeb, B. Carré, H. G. Muller, P. Agostini, and P. Salières, "Attosecond synchronization of high-harmonic soft X-rays," Science **302**, 1540–1543 (2003).
30. J. Tate, T. Auguste, H. G. Muller, P. Salières, P. Agostini, and L. F. DiMauro, "Scaling of wave-packet dynamics in an intense midinfrared field," Phys. Rev. Lett. **98**(1), 013901 (2007).
31. G. Doumy, J. Wheeler, C. Roedig, R. Chirla, P. Agostini, and L. F. DiMauro, "Attosecond synchronization of high-order harmonics from midinfrared drivers," Phys. Rev. Lett. **102**(9), 093002 (2009).
32. P. Salières and I. Christov, "Macroscopic effects in high-order harmonic generation," in *Strong Field Laser Physics*, Thomas Brabec, ed. (Springer, 2009).
33. V. P. Kalosha and J. Herrmann, "Formation of optical subcycle pulses and full Maxwell-Bloch solitary waves by coherent propagation effects," Phys. Rev. Lett. **83**, 544–547 (1999).
34. R. W. Ziolkowski, J. M. Arnold, and D. M. Gogny, "Ultrafast pulse interactions with two-level atoms," Phys. Rev. A **52**, 3082–3094 (1995).
35. R. Pan, "Few-cycle ultrashort pulse laser propagation in organic molecular material," Acta Sinica Quantum Optica **17**, 52–57 (2011).
36. J. Xiao, Z. Wang, and Z. Xu, "Area evolution of a few-cycle pulse laser in a two-level-atom medium," Phys. Rev. A **65**, 031402 (2002).
37. K. Xia, S. Gong, C. Liu, X. Song, and Y. Niu, "Near dipole-dipole effects on the propagation of few-cycle pulse

in a dense two-level medium," Opt. Express **13**, 5913–5924 (2005).
38. P. Hu, Y. Niu, Y. Xiang, and S. Gong, "Above-threshold ionization by few-cycle phase jump pulses," Opt. Express **21**, 24309–24317 (2013).
39. P. Hu, Y. Niu, Y. Xiang, S. Gong, and C. Liu, "Carrier-envelope phase dependence of molecular harmonic spectral minima induced by mid-infrared laser pulses," Opt. Express **21**(20), 24309–24317 (2015).
40. X.-M. Tong and S.-I. Chu, "Probing the spectral and temporal structures of high-order harmonic generation in intense laser pulses," Phys. Rev. A **61**, 021802(R) (2000).
41. K. S. Yee, "Numerical solution of initial boundary value problems involing Maxwell's equations in isotropic media," IEEE Trans. Antennas Propag. **14**, 302–307 (1966).
42. G. Mur, "Absorbing boundary conditions for the finite-difference approximation of the time-domain electromagnetic-field equations," IEEE. Trans. Electronmagn. Compat. **EMC-23**, 377–382 (1981).

1. Introduction

Femtosecond laser technology has obtained rapid development over the past decades, and it provides us important tools to study the strong-filed physics as well as the ultrafast phenomena. People can observe the ultra-fast dynamic chemical reaction process using the femtosecond technology, such as, the breaking and restructuring of the chemical bond [1] and the vibrations of an atom or a molecule [2]. However, if we want to observe further faster physical phenomena, such as electron motion, the sub-femtosecond or attosecond pulse should be used [3]. In recent decades, one important and effective method to generate an attosecond laser pulse is the Fourier synthesis to the high-order harmonics. Krausz's team has first obtained the sub-femtosecond pulse output (650 as) in experiment in 2003 [4]. From then on, this method gained extensive attention. Especially, Krausz's team obtained an 80 as pulse by utilizing a 3.3 fs driving laser pulse, which broke the limit of 100 as [4].

As for the high-order harmonic generation (HHG), it is first proposed by Shore and Knight in 1987 [5], and subsequently, observed experimentally by McPherson [6] and Farray [7]. Its intuitive physical mechanism can be summarized as a *three-step* model proposed by Corkum first [8] and developed by Lewenstein *et al.* later [9]: first, electrons are liberated from the parent ion via tunneling ionization, then they move away and acquire energy from the laser field, finally small part of them may return back to the parent ion and recombine to the ground state with a harmonic photon emitted. The whole HHG spectrum has a unique character: the first few harmonics decay exponentially rapidly followed by a plateau in which the harmonic intensity varies weakly with order, and eventually an abrupt cut-off occurs [10]. Later, people found that HHG can also occur with no electron ionized. For a two-level atomic system, if the driving laser field is not so strong and the frequency is much less than the atomic energy level transition frequency, a HHG process can be demonstrated and the corresponding HHG spectrum also process a long generic plateau and clear cutoff [11–14]. This kind of HHG has no connection with the above mentioned *three-step* model. Its origin is clarified by Gauthey *et al.* [14] as is linked to the rapid level crossing at each half-cycle of the laser period and the cutoff position analytically presented under a driven two-level model is in a good agreement with the numerical simulation result. Later, Faria *et al.* [15] extended this two-level model with an analogous *three-step* model to explain the harmonic generation process: a population transfer occurs from the field-dressed adiabatic lower state to the upper state at level crossing time, then the system acquires energy from the laser field, finally decays back to the lower state and radiates a harmonic photon with the energy equaling to the transient transition energy separation.

Fourier transform to the harmonics within the plateau or the cut-off part of the spectra referring filtering or other technology is a routine tool to make an attosecond pulse train (APT) or isolated attosecond pulse (IAP) generated. Since the HHG spectra is sensitive to the driving laser pulse, quantum control schemes for high quality IAP or APT obtaining have been demonstrated widely, such as polarization gating [8, 16], nonlinear chirped laser pulse [17], two-color

laser pulse [18], and some kind of combination of these methods [19], etc.. In the driven two-level regime, the two-color laser pulse [20–22] has been demonstrated, and it is found that the plateau can be extended. The polar molecule system demonstrated that the existence of permanent dipole moment can significantly extend the spectrum plateau (even to X-ray range) [23]. Moreover, if a hyperbolic tangent chirped few-cycle laser pulse is used to drive a two-level quantum well, an ultra-broad super-continuum can be obtained and can be used to synthesize an isolated terahertz pulse [24]. Therefore, this paper proposes that one can control the matter and the driving laser pulse at the same time. The plateau extension is expected with the help of permanent dipole moment, meanwhile, coherent enhancement for the HHG spectrum is expected by modulating the laser pulse with a chirp.

Actually, almost all the studies about HHG based on the driven two-level model just considered the single-particle-response, namely, the two-level system is only one atom, one molecule or one quantum well, etc. However, there are thousands of particles and the laser pulse and generated harmonic will propagate through the medium in the real experiment. As we know, in the ionization regime, if the driving pulse and the harmonic have the same phase velocity as they travel through the medium, the harmonic signal will achieve significant increase [32]. Many studies based on the driven two-level model with dense medium also have been done [33–37], however, their focus is mainly concentrated on the modulation of the laser pulse during the propagation process. Therefore, the macroscopic propagation process will be investigated in this paper and is expected to enhance the harmonic signal.

2. Theoretical models and methods

For the two cases of propagation considered or not, both the simulation model and the numerical solving method are different. In simple terms, here, non-propagation case need to solve the nonlinear Bloch equations by Runge-Kutta method and the propagation case need to solve the Maxwell-Bloch equations by finite-difference time-domain (FDTD) method. The two models and their corresponding solving methods will be introduced separately.

First for the non-propagation case. Consider a two-level system where $|1\rangle$ and $|2\rangle$ represent the ground and excited states with the energy separation ω_0 [Atomic units (a.u.) are used in this paper, unless otherwise mentioned]. Within this picture, the time-dependent wave function is

$$|\Psi(t)\rangle = c_1(t)|1\rangle + c_2(t)|2\rangle, \tag{1}$$

where $c_{\mathrm{i}}(t) = \langle \mathrm{i}|\Psi(t)\rangle\,(\mathrm{i}=1,2)$ denotes the overlap of the total wave function with the i^{th} state.

A semi-classical model is adopted in which the quantum system interacts with the classical laser field. The total Hamiltonian describing the interaction of the laser field with the two-level system which has permanent dipole moments is [23]

$$H = H_0 + V = \begin{pmatrix} E_1 & 0 \\ 0 & E_2 \end{pmatrix} - E(t)\begin{pmatrix} \mu_{11} & \mu_{12} \\ \mu_{21} & \mu_{22} \end{pmatrix}, \tag{2}$$

where μ_{ij} are the dipole moment matrix elements, and $E_1 = -\frac{1}{2}\omega_0$, $E_2 = \frac{1}{2}\omega_0$. The linearly polarized Gaussian pulse is used to drive the system and the laser field is given by expression of

$$E(t) = E_0 \exp\left[-4\ln 2(t/\tau)^2\right]\cos\left[\omega_L t + \varphi(t)\right], \tag{3}$$

where E_0 is the field amplitude, τ is the duration (full width at half maximum, FWHM), ω_{L} is the field angular frequency, and $\varphi(t)$ is the time-dependent carrier envelope phase.

Finally, the system dynamics can be described by the following nonlinear Bloch equations:

$$\partial_t u(t) = \omega_0 v(t) + 2\xi\Omega(t) v(t), \tag{4}$$

$$\partial_t v(t) = -\omega_0 u(t) + 2\Omega(t) w(t) - 2\xi\Omega(t) u(t), \tag{5}$$

$$\partial_t w(t) = -2\Omega(t) v(t). \tag{6}$$

Where, $u(t)$ and $v(t)$ are the mean real and imaginary parts of polarization, respectively, $w(t)$ is the mean population difference. $\Omega(t) = -\vec{\mu}_{21}\vec{E}(t) = \Omega_0/E_0 \cdot E(t)$ is the Rabi frequency of the incident laser field with peak value of $\Omega_0 = -\mu_{21}E_0$, $\xi = (\mu_{22} - \mu_{11})/2\mu_{21}$ is a dimensionless parameter which characterizes the permanent dipole moment. In the two-level model, the main observable of interest is $u(t)$, which leads to the coherent part of the light spectrum by Fourier transform

$$P(\omega) = \left|\mathrm{d}t \exp(i\omega t)\bar{N}u(t)\right|^2. \tag{7}$$

Where $\bar{N}$ is density of the medium, it is introduced here for the consistency with propagation situation discussed later. It is chosen as $\bar{N} = 7.5 \times 10^{24}\mathrm{m}^{-3}$ for both the propagation and non-propagation cases. The system of evolution Eqs. (4)–(6) can be solved numerically without making rotating-wave approximation by means of a fourth-order Runge-Kutta method. The Fourier transform is performed using the Fast Fourier transform algorithm.

Moreover, the time-frequency analysis is performed to the high-order harmonic generation by using the wavelet transform to the induced dipole moment $u(t)$ in order to investigate the temporal structures of HHG spectrum,

$$A_\omega(t,\omega) = \int \bar{N}u\left(t'\right)\sqrt{\omega}W\left[\omega\left(t-t'\right)\right]\mathrm{d}t', \tag{8}$$

where $W(x)$ is the window function (also called the mother wavelet function) which is given here by the form of Morlet wavelet [24, 38–40]

$$W(x) = \sqrt{\frac{1}{\tau_{wav}}}e^{ix}e^{-x^2/2\tau_{wav}^2}, \tag{9}$$

t and ω denote the time and harmonic frequency at which the window function is centered. The envelope width τ_{wav} of the wavelet is set to 6.0 in our calculations.

As for the propagation case, the Maxwell-Bloch equations should be numerically solved. Now, propagation of a linearly polarized short laser pulse along the z axis to an input interface of the two-level medium at $z = L_1$ is considered. Initially the pulse propagates in the vacuum of free space, then it penetrates into the medium with some reflects, the penetrating part propagates through the medium and finally exits again into the vacuum through the output interface at $z = L_2$ [33]. If the laser field is assumed to polarize along the x axis, then the Maxwell-Bloch equations would take the form of

$$\begin{aligned}
&\partial_t H_y(z,t) = -\tfrac{1}{\mu_0}\partial_z E_x(z,t)\ , \\
&\partial_t E_x(z,t) = -\tfrac{1}{\varepsilon_0}\partial_z H_y(z,t) - \tfrac{1}{\varepsilon_0}\partial_t P_x(z,t)\ , \\
&\partial_t u(z,t) = \omega_0 v(z,t) + 2\xi\Omega(z,t) v(z,t) - u(z,t)/T_2, \\
&\partial_t v(z,t) = -\omega_0 u(z,t) + 2\Omega(z,t) w(z,t) - 2\xi\Omega(z,t) u(z,t) - v(z,t)/T_2, \\
&\partial_t w(z,t) = -2\Omega(z,t) v(z,t) - [w(z,t) - w_0]/T_1.
\end{aligned} \tag{10}$$

Here E_{x}, H_{y} is the laser pulse electric and magnetic field, respectively. μ_0 and ε_0 are the vacuum permeability and vacuum permittivity, respectively. w_0 is the initial population difference. Maxwell equations are united with the Bloch equations here, and the physical quantities are not

only dependent on the time but also dependent on the propagation distance, z. Here the relaxation time of the two-level medium is considered, where T_1 is the excited-state lifetime and T_2 is the dephasing time. It is noted that, for the non-propagation case, the relaxation time are not considered because of that they are much longer than the laser-matter interaction time. P_{x} is the macroscopic nonlinear polarization, and is given for two-level system as expression of [35]

$$\begin{aligned} P_x &= \bar{N} tr\left(\vec{\mu}\rho\right) \\ &= \bar{N}\left(\mu_{11}\rho_{11} + \mu_{22}\rho_{22} + \mu_{12}\rho_{12} + \mu_{21}\rho_{21}\right) \end{aligned} \tag{11}$$

where $\bar{N}$ is the density of the medium, $\rho_{\mathrm{ij}}\,(\mathrm{i,j} = 1,2)$ is the density matrix element for the two-level system. If the system is closed (i.e., the system has no energy exchange with the outside environment), P_{x} can be further expressed as

$$P_x = \bar{N}\mu_{21}u + \bar{N}\xi\,\mu_{21}w + \bar{N}\left(\mu_{11} + \mu_{22}\right)/2. \tag{12}$$

Eq. (10) can be solved using Yee's leap-frog FDTD discretization scheme [41] with the iterative predictor-corrector method [34]. Mur absorbing boundary conditions [42] were incorporated with FDTD discretization which can avoid the unphysical reflection from the finite calculation boundaries. Here, the initial pulse condition is given as

$$\begin{aligned} E_x\left(z, t=0\right) &= E_0 \exp\left[-4\ln 2\left(\tfrac{z-z_0}{c\tau}\right)^2\right]\cos\left[\omega_L\left(z-z_0\right)/c\right], \\ H_y\left(z, t=0\right) &= \sqrt{\varepsilon_0/\mu_0}E_x\left(z, t=0\right), \end{aligned} \tag{13}$$

where c is the light velocity in the vacuum. The choice of z_0 can ensure that the pulse penetrates negligibly into the medium at $t = 0$. In our calculations z_0 is set to be 15 μm.

3. Results and discussions

First, the non-propagation case is discussed, as is generally done [13–15, 18, 20–24]. The two-level system with an energy separation $\omega_0 = 0.30$ a.u. is assumed initially in its ground state, then $u(0) = v(0) = 0$, and $w(0) = -1$. In addition, the dipole moment matrix element is $\mu_{21} =$ 1.18 a.u. (corresponds to 1.0×10^{-29}Asm) and no permanent dipole moment exists for the present. As for the driving laser pulse, its center frequency $\omega_{\mathrm{L}} = 0.056$ a.u. corresponding to a wavelength of 814 nm, its duration $\tau = 2T$ (about 5.43 fs, T is the laser period) and its peak Rabi frequency $\Omega_0 = 0.30$ a.u..

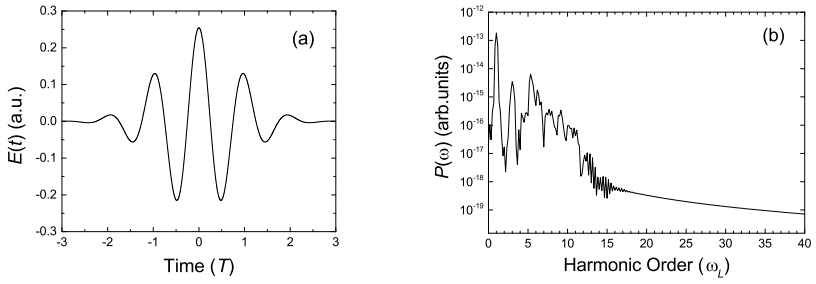

Fig. 1. (a) Non-chirped Gaussian laser pulse, and (b) the corresponding HHG spectrum of the driven two-level system without a permanent dipole moment. Parameters for this laser pulse are set as: central frequency $\omega_L = 0.056$ a.u., duration $\tau = 5.43$ fs, and peak Rabi frequency $\Omega_0 = 0.30$ a.u..

It has been well clarified that, as for a two-level atomic system, the occurrence of HHG is attributed to the rapid level crossing mechanism between the two field-dressed adiabatic states [14]. In the adiabatic basis, the Hamiltonian is diagonalized via a unitary transformation as,

$$\tilde{H} = \hat{U} H \hat{U}^{\dagger} = \begin{pmatrix} \varepsilon_{-} & 0 \\ 0 & \varepsilon_{+} \end{pmatrix}, \tag{14}$$

with the field-dressed level energies [23]

$$\varepsilon_{\pm} = \frac{1}{2}\left(-\frac{\mu_{11}+\mu_{22}}{\mu_{21}}\Omega(t) \pm \sqrt{[2\xi\Omega(t)-\omega_0]^2 + [2\Omega(t)]^2} \right). \tag{15}$$

and the frequency of harmonic emitted at time t is determined by the transient energy separation of these two states,

$$\omega = \varepsilon_{+} - \varepsilon_{-} = \sqrt{[2\xi\Omega(t)-\omega_0]^2 + [2\Omega(t)]^2} = N\omega_L. \tag{16}$$

Where, N is the harmonic order. Formula (16) clearly indicates that the harmonic frequency varies over time and would have a maximum value $\omega_{\max}$ with a cutoff order $N_{\max}$ at time $t_{\max}$ which can be found with the help of the $\omega - t$ plot curve. If the two-level system has no permanent dipole moment existing, that is, $\xi = 0$, and the driving laser pulse is not chirped [Fig. 1(a)], the numerical obtained HHG spectrum is shown in Fig. 1(b). It possesses the generic characteristics of a HHG spectrum: a plateau and a clear cutoff. The cutoff order is 11, which agree well with the predicted value $N_{\max}$.

Now, if a permanent dipole moment is introduced, as shown in Fig. 2, the corresponding HHG spectrum will change significantly, even though the other laser and two-level system parameters remain unchanged. For example, if the permanent dipole moment is $\mu_{11} = -4\mu_{21}$, $\mu_{11} = 4\mu_{21}(\xi = 4)$ as shown in Figs. 2(a) and 2(e), the cutoff harmonic order is extended to be about 40th, which also agree well with the prediction value $N_{\max}$ by Eq. 16. If the permanent dipole moment is large enough [e.g., $\mu_{11} = 0$, $\mu_{11} = 16\mu_{21}(\xi = 8)$], the cutoff order can be further extended to the soft X-ray range, which would provide a possibility to generate a much shorter IAP or APT by synthesizing much more harmonics. It is found from the comparison of Figs. 2(e) and 2(f) that, the harmonic generation process is sensitive to the direction of initial permanent dipole moment: for negative ξ (here we call it the negative direction), the cutoff harmonic is emitted only at laser field peak time, while for positive ξ (the positive direction), it is emitted at both sides of the peak with about $0.5T$ interval to the peak time. This result can also be deduced from Eq. 16. In addition, Figs. 2(e) and 2(f) clearly demonstrate that, as Ref. [24] says, the time-frequency HHG spectrum shares the same shape with the laser pulse absolute amplitude. Even though there's little difference existing for the case of positive initial permanent dipole moment (positive ξ), but at least the minimum and peak time of the time-frequency spectrum are totally same with those of the laser pulse absolute amplitude.

However, we note that and it can be seen from Figs. 2(e) and 2(f) that, even though the harmonic cutoff energy can be largely extended, the HHG spectra exhibit more than five well-formed individual peak structures in the plateau region, which means that the plateau harmonics have more than ten generated trajectories. If one select these plateau harmonics to synthesize an attosecond pulse, there're would have about ten individual peaks. That is an APT. However, people have been dedicated to obtain an IAP with short duration for many years [16, 25–28] . Therefore, if the plateau harmonic's trajectory number can be reduced, an APT with less peaks even an IAP may be generated. In the following of this paper, a nonlinear chirped frequency is introduced to the driving laser pulse and is expected to reduce the trajectory number.

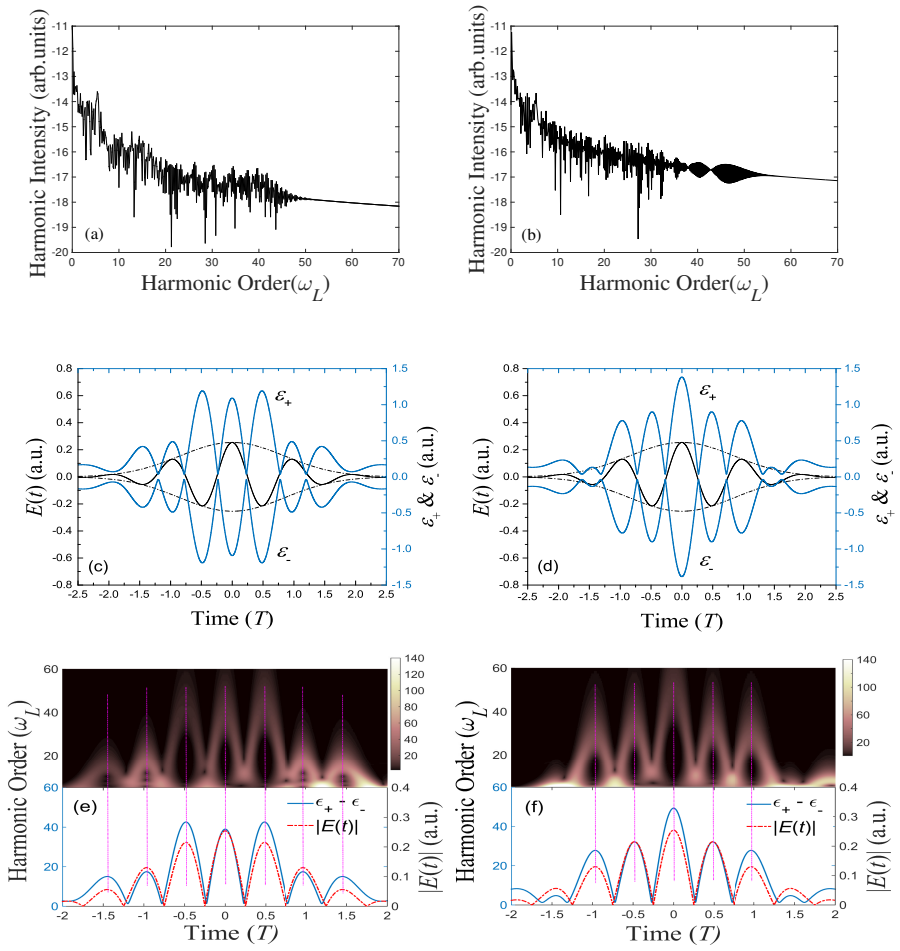

Fig. 2. HHG spectra of a laser-driven two-level system with a permanent dipole moment existing, of (a) $\mu_{11} = -4\mu_{21}, \mu_{22} = 4\mu_{21} (\xi = 4)$, (b) $\mu_{11} = 4\mu_{21}, \mu_{22} = -4\mu_{21} (\xi = -4)$. (c) and (d) show the corresponding time-dependent eigenvalue of the two dressed states ε_+ and ε_-. (e) and (f) show their corresponding time-frequency spectra via wavelet transforms, while the lower panel displays the time-dependent energy separation between the two dressed states $\varepsilon_+ - \varepsilon_-$ (the harmonic energy predicted by two-level model) and the absolute amplitude of laser field. The other laser and two-level system parameters are same with those in Fig. 1.

The chirp chosen is with a hyperbolic tangent form [17], and the time-dependent carrier envelope phase $\varphi(t)$ in Eq. (3) is then written as:

$$\varphi(t) = -\eta \tanh\left[(t - t_d)/\tau_c\right]. \tag{17}$$

Where τ_c is the steepness of the chirp function and t_d is set at the middle of the sweep here. η denotes the frequency sweeping range. If $\eta = 0$, driving pulse is chirp free. With a chirp, compared to the laser pulse shown in Fig. 1(a), the temporal shape of the laser pulse changes significantly (Fig. 3), and its origin oscillatory periodicity and up-down symmetry disappear: the central part of the carrier wave gets broader, the side parts become weaker, while the peak

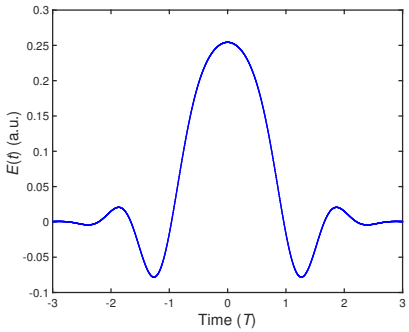

Fig. 3. The laser pulse with chirped frequency. $\eta = 6.25$, $\tau_c = 120$, the other laser parameters are the same with those in Fig. 1(a).

amplitude is remained. Importantly, the introduce of chirp makes the absolute amplitude difference between the pulse central peak and its neighbored ones get larger. According to the rapid level crossing theory, the time-frequency HHG spectrum shares the same shape with the absolute laser pulse amplitude [24]. Therefore, if the initial permanent dipole moment ξ is negative, it's easy to speculate that the HHG spectrum would have a large plateau whose harmonics have only two generation trajectories at most. This is much less than that of the case without chirp shown in Figs. 2(e) and 2(f). Thus, an APT with only two peaks can be generated by synthesizing the plateau harmonics. However, it can be seen from Figs. 1(a) and 3 that, the introduce of chirp has weakened steepness of the laser pulse peak's rising and falling edges because of the increase of time interval between the peak time and its adjacent zero time which results from the getting broader of the center carrier. As mentioned before, the time-frequency HHG spectrum shares the same shape with the laser pulse absolute amplitude. Therefore, this steepness weakening could lead to the enlargement of atto-chirp [29–31] for both trajectories which can increase the FWHM for both peaks of generated APT. However, it is contradictory for the center carrier to get narrower and for the absolute amplitude difference between the pulse central peak and its neighbored ones to get larger. Thus, a proper group of chirp parameters are chosen here as $\eta = 6.25,\ \tau_c = 120$, which can make the absolute amplitude difference quite large and the center carrier not too broad, just as shown in Fig. 3.

Fig. 4(a) shows the HHG spectrum of the two-level system with a permanent dipole moment $[\mu_{11} = 4,\ \mu_{22} = -4(\xi = -4)]$ driven by a chirped laser pulse. Compared to the case of Fig. 2(b) the only difference is the introduce of the chirp. The corresponding time-frequency profile of the harmonic spectrum is shown in Fig. 4(b). Since the initial permanent dipole moment is negative, the cutoff harmonic must emit at the laser pulse peak time. In addition, the introduce of chirp doesn't change the laser pulse envelope (E_0 and Ω_0 remain invariant). According to Eq. 16, the harmonic spectra should have the same cutoff energy as the case shown in Figs. 2(b), 2(f). This is confirmed by the numerical results in Figs. 4(a) and 4(b). Because of the pulse shape changes mentioned before, there are only three well-formed individual peak structures besides the central peak in the time-frequency spectrum while the case without chirp has six ones. Moreover, these peak values are much smaller than those of case without chirp, this makes the value difference between the central peak and the sub-peak much larger than that of without chirp case shown in Fig. 2(f). Therefore, the harmonics would have two generation trajectories at most within such a large plateau region. Therefore, one can use harmonics within this region to synthesize an APT with only two individual peaks.

Next, harmonics generated from the system with a permanent dipole moments $[\mu_{11} =$

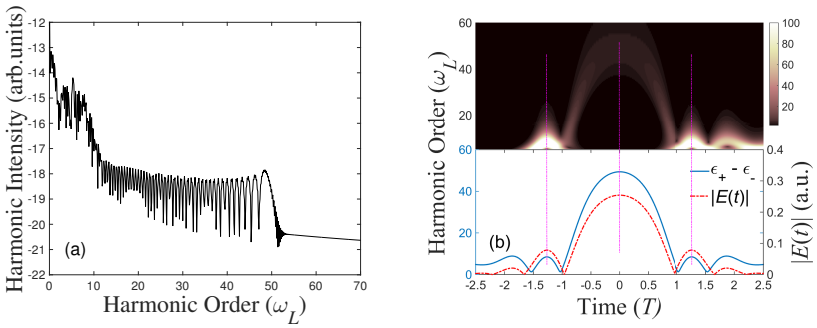

Fig. 4. (a) HHG spectrum and (b) its corresponding wavelet time-frequency analysis for a chirped-laser-driven two-level system with a permanent dipole moment [$\mu_{11} = 4$, $\mu_{22} = -4(\xi = -4)$]. The lower panel of figure (b) shows time-dependent energy separation between the two dressed states $\varepsilon_+ - \varepsilon_-$ (the harmonic energy predicted by two-level model) as in Fig. 2(e) and 2(f). The other laser and two-level system parameters are same with those in Fig. 2.

4, $\mu_{22} = -4(\xi = -4)$] within the plateau region are selected to synthesize attosecond pulses for both cases with and without chirp. All the harmonics (including the even orders) from 14th to 29th are selected for both cases. The results are shown in Figs. 5(a) and 5(b), respectively. Every FWHM of all peaks is marked in the figures. There is an APT generated with ten individual peaks for the case without chirp, while there is an APT generated which has only two individual peaks (we call it attosecond pulse pair, APP). This is completely consistent with the trajectory numbers in the plateau region (shown in Figs. 2(f) and 4(b)). Therefore, we have successfully reduced the individual peak numbers of the generated APT by introducing chirp frequency to the driving laser pulse. However, there is no IAP generated. In addition, the increase of two FWHMs for both two center peaks confirms that the chirp frequency could enlarge the attochirp.

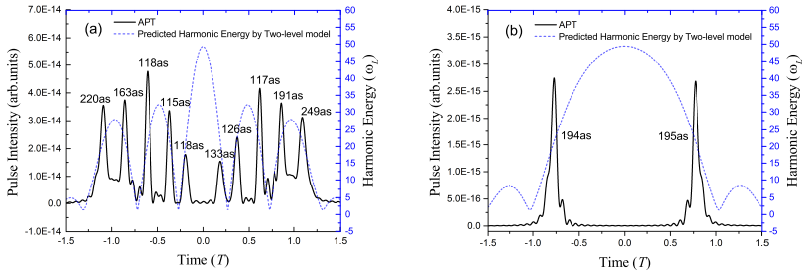

Fig. 5. Generated attosecond pulse train (APT) by synthesizing plateau harmonics (from 14th to 29th) driven by a laser pulse (a) without chirp and (b) with chirp. The other laser and two-level system parameters are same with those in Fig. 4. The blue dashed curve is the harmonic energy predicted by the two-level model same with Figs. 2(e) and 2(f).

Thus we have demonstrated that the combination of controls, introduce of permanent dipole moment to two-level system and chirp frequency to driving laser pulse, has big influences on the HHG and attosecond pulse generation process. Due to the permanent dipole moment, much more plateau harmonics are generated and used to synthesize a shorter attosecond pulse; on

the other hand, the chirp frequency could reduce the generation trajectory numbers of plateau harmonics to a minimum of two which can finally lead to an APP generated. However, the pulse intensity is much weaker than that of the case without chirp (seen in Fig. 5). In view of this, a method that could enhance the harmonic signal intensity should be proposed to make up the intensity loss for introducing the chirp frequency. Here, we will investigate the propagation conditions and expect it can enhance the harmonic intensity. One part medium parameters are chosen as: , $T_1 = 1.0 \times 10^{-12}$s, $T_2 = 0.5 \times 10^{-12}$s [33] and the other medium and all the laser parameters are all the same with those of non-propagation cases in Fig. 5. Initial condition of the laser pulse was given in part *theoretical models and methods*. As for the chirped laser pulse, the initial condition is

$$\begin{aligned} E_x(z,t=0) &= E_0 \exp\left[-4\ln 2\left(\tfrac{z-z_0}{c\tau}\right)^2\right] \cos\left[\omega_L(z-z_0)/c + \eta \tanh\tfrac{z-z_0}{c\tau_c}\right], \\ H_y(z,t=0) &= \sqrt{\varepsilon_0/\mu_0} E_x(z,t=0). \end{aligned} \tag{18}$$

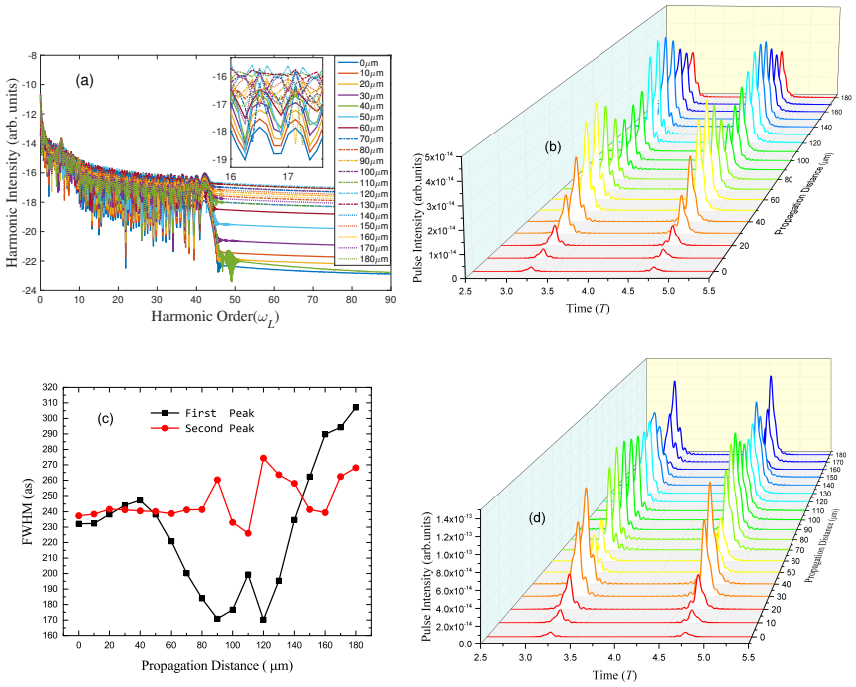

Fig. 6. (a) Nineteen groups of harmonic spectra corresponding to nineteen groups of propagation distance. (b) Generated APPs by synthesizing plateau harmonics (between 14th to 29th) of spectra (a). (c) The FWHMs of generated APPs. (d) Nine groups of generated APPs for medium with a larger density of $\bar{N} = 12.5 \times 10^{24}\mathrm{m}^{-3}$ (harmonics selected from 14th to 29th). Two-level system has a permanent dipole moment of $\mu_{11} = 4$, $\mu_{22} = -4(\xi = -4)$. The laser pulse and other two-level system parameters are same with those of Fig. 5.

Nineteen groups of propagation distance are investigated from 0 to 180 μm evenly divided by 10 μm, and harmonic generation in the transmission interface will be studied, respectively. The simulation results are shown in Fig. 6, including the HHG spectra, generated APPs, and the FWHMs. The same plateau harmonic orders (14th to 29th) are selected to synthesize the APP. The HHG spectra demonstrated that the propagation distance has a big influence on the

plateau harmonic intensity. However the intensity is not linearly changed with propagation distance. The inset in Fig. 6(a) shows that at first the plateau harmonic intensity gradually increase to a maximum value, then decrease to a minimum value, after that it will process another increase and decrease process and so on. This process can be verified in Fig. 6(b) which clearly shows that the generated APP's intensity oscillates with propagation distance change. In our simulations, the maximum values appear at 60μm and 130μm. They are about ten times that of the non-propagation case. The FWHM is studied for two peaks of each APP, and it also changes with propagation distance variation. The change range is about 140as from 170as to 310as in our simulations. The minimum FWHM 170as appears at about 120μm. We note that, for distances 60μm and 130μm, their pulse peaks FWHMs have an average about 220as which is not much longer than that of the non-propagation case. Therefore, we demonstrated that it can dramatically enhance the plateau harmonic intensity if a proper propagation distance is considered. In addition to this, the medium density is also studied. We increased it to $\bar{N} = 12.5 \times 10^{24}\mathrm{m}^{-3}$, and the corresponding APPs are shown in Fig. 6(d). It shows that the maximum values appear at about 40μm, 90μm and 140μm. The distance between adjacent is about 50μm. It is about 20μm less than that of the case of smaller medium density $\bar{N} = 7.5 \times 10^{24}\mathrm{m}^{-3}$. Therefore, one can use dense medium to propagate a shorter distance or use sparse medium to propagate a longer distance to enhance the harmonic intensity.

4. Conclusions

In this paper, we tried to combine the control of the matter and the control of the driving laser pulse to produce a high-order harmonic spectrum with a higher cutoff energy. It is shown that the existence of the permanent dipole moments can significantly extend the plateau of the harmonic spectrum. However, the plateau harmonic has more than two generated trajectories, which can not generate an IAP by synthesizing harmonics within this region. If the laser pulse is chirped, the up-down symmetry of the laser field will be dramatically changed. This kind of laser pulse can exactly reduce the trajectories to a minimum of two. Although there still an IAP generated, an APT with only two individual peaks (APP) is obtained by Fourier synthesis harmonics within the plateau region. If the propagation effect is considered, it can dramatically enhance the plateau harmonic intensity (maximum of about 10 times) for a proper propagation distance.

Acknowledgments

This work is supported by the National Natural Science Foundation of China (NNSF, Grant No.11374318). C.L. appreciates the supports from the 100-Talents Project of Chinese Academy of Sciences and Department of Human Resources and Social Security of China.